A paleomagnetic study of Permian and Triassic rocks from the Toulon-Cuers Basin, SE France: Evidence for intra-Pangea block rotations in the Permian

K. Aubele,[1] V. Bachtadse,[1] G. Muttoni,[2] A. Ronchi,[3] and M. Durand[4]

Received 19 September 2011; revised 10 April 2012; accepted 17 April 2012; published 12 June 2012.

[1] The identification of a massive shear zone separating Gondwana from Laurasia during late Palaeozoic times is one of the prerequisites for the controversial Pangea B to A transition. Here we present new paleomagnetic data from Permian and Triassic sediments and volcanic rocks from the Toulon-Cuers basin, SE France, likely to be situated within this intra-Pangea shear zone. A total of 150 samples from 14 sites were collected in the field; 108 samples yielded reliable paleomagnetic component directions based on stepwise thermal demagnetization up to maximum temperatures of 690°C. After removal of an initial viscous magnetic component from room temperature up to 200°C, a second component of reverse polarity, oriented to the south-and-up, was identified in almost all samples of Permian age. The Triassic samples behave similarly, with the notable difference that here, two polarities of magnetization are present. Positive field tests suggest the primary character of this characteristic magnetization. The latitudes of the resulting Early to Mid Permian paleopoles agree well with the corresponding segment of the apparent polar wander path (APWP) for Europe, whereas the longitudes are strung out along a small circle segment, indicating relative rotations between the sampled regions and stable Europe. The Triassic poles, instead, plot close to the Triassic segment of the European APWP and provide an upper time limit for the observed rotations. These results suggest a wrench faulting event associated with intra-Pangea crustal instability and transformation during the Permian.

Citation: Aubele, K., V. Bachtadse, G. Muttoni, A. Ronchi, and M. Durand (2012), A paleomagnetic study of Permian and Triassic rocks from the Toulon-Cuers Basin, SE France: Evidence for intra-Pangea block rotations in the Permian, *Tectonics*, *31*, TC3015, doi:10.1029/2011TC003026.

1. Introduction

[2] The Variscan amalgamation of Laurasia and Gondwana was followed by a late Paleozoic period of Pangea instability and reconfiguration. In their classic study on strike-slip faulting in Europe and northern Africa, *Arthaud and Matte* [1977] point out the existence of a Late Carboniferous–Early Permian right lateral shear system connecting the Appalachians to the Urals, with the central part of this intra-Pangea shear system being presumably located between the Iberian Peninsula and the Bohemian massif (Figure 1). Within this tectonic setting, the High Atlas fault, the Biscay-North Pyrenean fault, and the South Armorican shears in Brittany [see also *Bard*, 1997] acted as first-order wrench faults. Based on the original observations made by *Arthaud and Matte* [1977], *Muttoni et al.* [1996, 2003] suggested that this episode of intra-Pangea wrench faulting was followed by the transformation of Pangea from an Early Permian configuration termed B after *Irving* [1977], characterized by South America and Africa located to the south of Europe and Asia, respectively, to a Late Permian Wegenerian A-type configuration by way of 3000 km of dextral displacement of Laurasia relative to Gondwana occurring essentially during the middle part of the Permian (Figure 2) [see *Muttoni et al.*, 2003]. However, the necessity to arrange Laurasia and Gondwana in a Pangea B configuration as opposed to the classic Wegenerian geometry has been challenged by several authors who questioned the quality of the palaeomagnetic data set for the Carboniferous and Permian and therefore the derived magnitude of the continental overlap between the two supercontinents at the basis of the Pangea B concept (see *Muttoni et al.* [2003], *Irving* [2005], and *Domeier et al.* [2012] for different views on the Pangea controversy).

[1]Department of Earth and Environmental Sciences, Ludwig-Maximilians-Universität München, Munich, Germany.
[2]Dipartimento di Scienze della Terra, Università di Milano, Milan, Italy.
[3]Dipartimento di Scienze della Terra, Università di Pavia, Pavia, Italy.
[4]Laxou, France.

Corresponding author: K. Aubele, Department of Earth and Environmental Sciences, Ludwig-Maximilians-Universität München, Theresienstr. 41, D-80333 Munich, Germany. (aubele@geophysik.uni-muenchen.de)

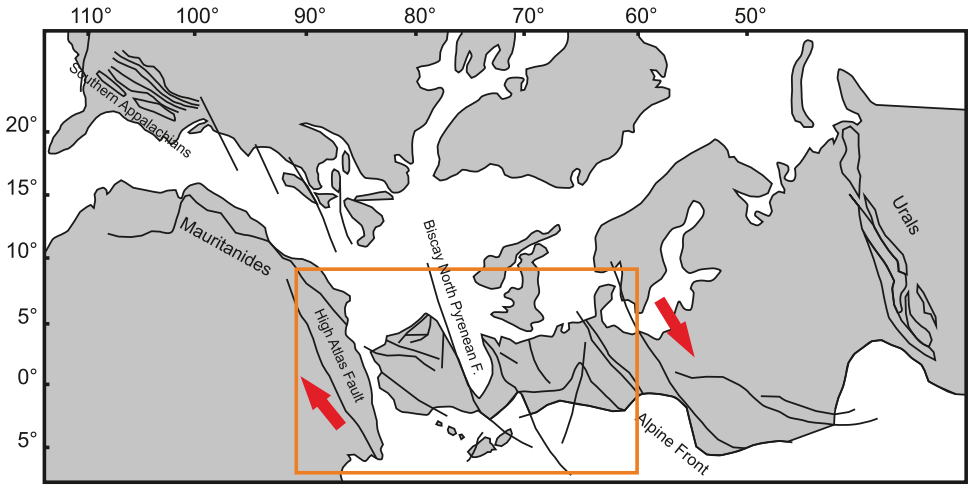

Figure 1. Location and outlines of the Pangea Transform Zone after *Arthaud and Matte* [1977].

[3] The continental-scale events of dextral shearing related to late Paleozoic Pangea instability should have left a fingerprint in the crustal structure of portions of southern Europe formerly located between Laurasia and Gondwana (Figures 1 and 2). For example, tectonic block rotations have been observed in Early Permian rocks from the French Massif Central, while Late Permian rocks from the same area are unrotated [*Chen et al.*, 2006, and references therein]; large rotations have also been documented in Late Carboniferous–Permian rocks from Maures-Estérel in southern France and from Corsica-Sardinia [*Edel*, 2000; *Emmer et al.*, 2005]; in Sardinia, recent paleomagnetic results indicate that these rotations should have occurred before Jurassic times [*Aubele et al.*, 2009; *Kirscher et al.*, 2011].

[4] Despite this growing body of knowledge, it is fair to say that the precise timing, geographic distribution, and triggering mechanism(s) of these block rotations are still poorly constrained. In order to enhance our knowledge on Permian deformation and block rotations in the Mediterranean, we carried out a paleomagnetic study on Permian-Triassic sediments and Permian volcanic rocks from the Toulon-Cuers region of southern France (see Figures 3 and 4).

2. Geological Setting

[5] In the course of the late Paleozoic period of crustal instability and re-equilibration of the European and African lithosphere, the Toulon-Cuers basin in SE Provence opened as a result of NE-SW directed crustal extension [*McCann et al.*, 2006].

[6] In the following paragraphs, the stratigraphic units of the Toulon-Cuers basin and the associated age estimates taken from the literature are described [*Durand*, 2001] (see the auxiliary material for detailed stratigraphic information).[1] Figure 4 (modified after *Durand* [2008]) summarizes the stratigraphic and numerical ages of the studied units after *Visscher* [1968], *Durand* [1988], *Demathieu and Durand*

[1]Auxiliary materials are available in the HTML. doi:10.1029/2011TC003026.

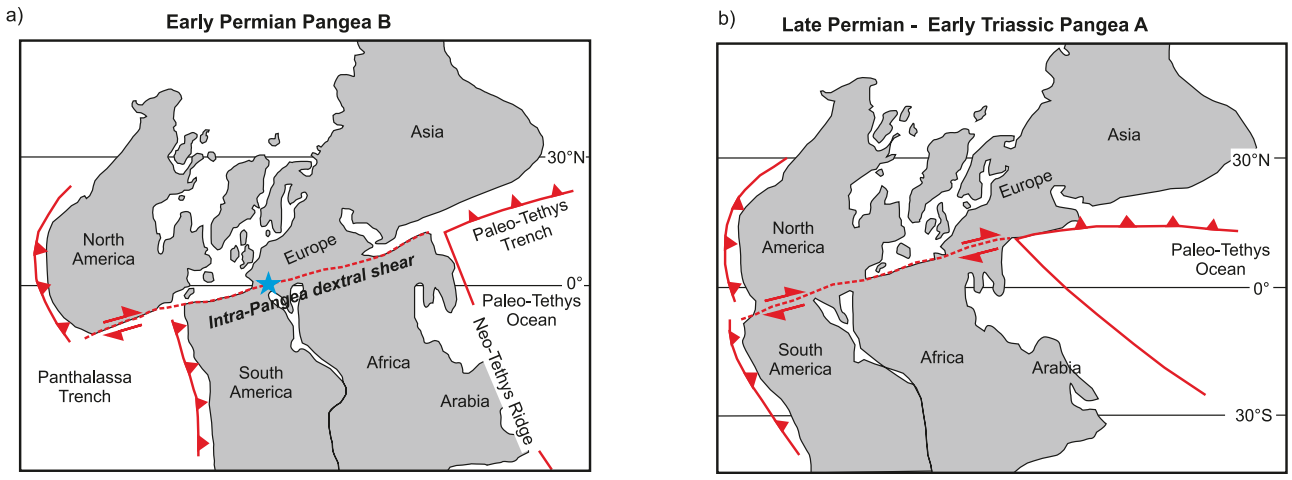

Figure 2. (a) Pangea B configuration after *Irving* [1977] in the Early Permian. (b) Wegenerian Pangea A configuration after *Muttoni et al.* [2003, 2004] in the Late Permian to Early Triassic. The blue star marks the study location in SW Europe. Modified after *Muttoni et al.* [2009].

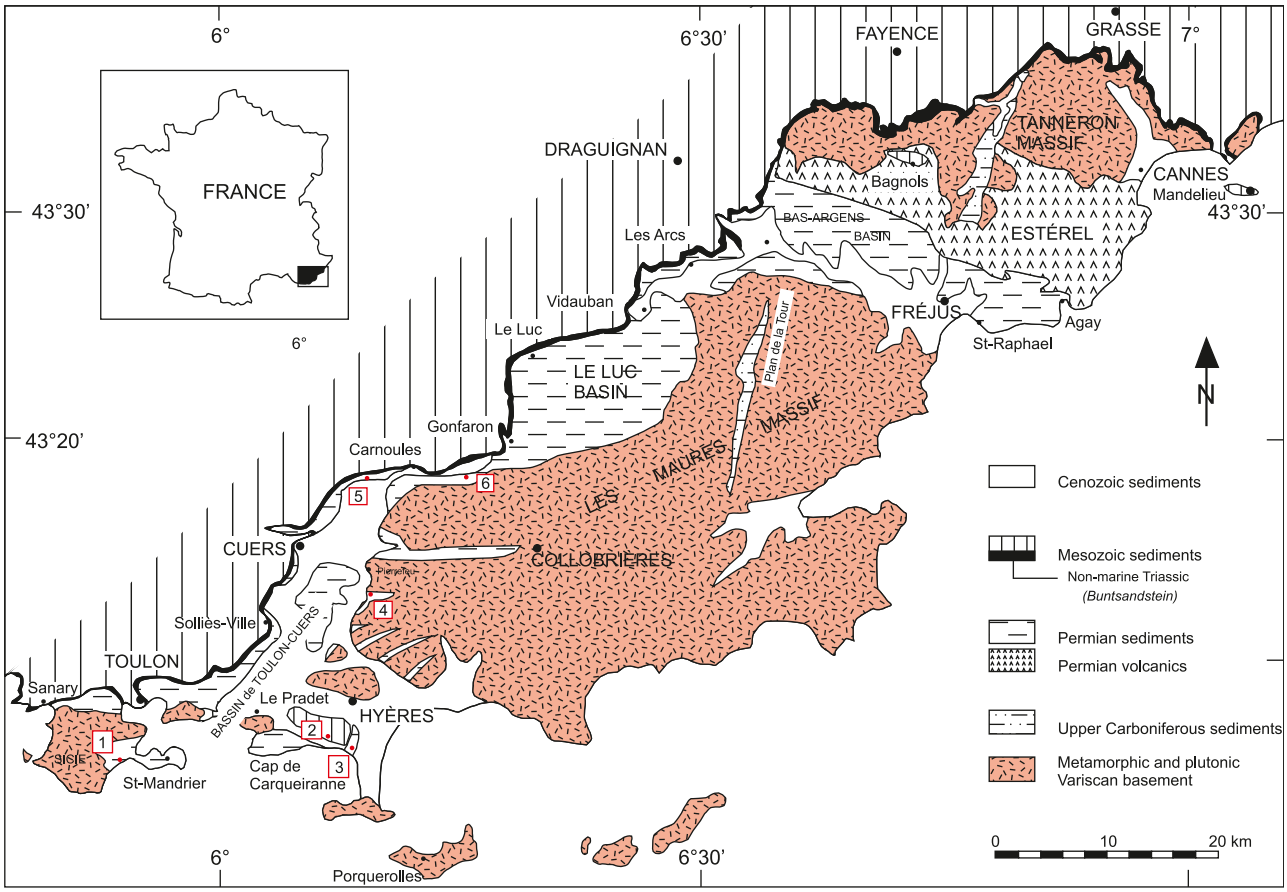

Figure 3. Geological outline of Provence, SE France including sample locations: (1) five sites within the Saint-Mandrier Fm., (2) three sites within the Grès de Gonfaron (sandstone), (3) three sites within the Les Salettes Fm., (4) sites within the LesPellegrins Fm. (rejected from the data set), (5) one site within the Bron Fm. near Carnoules, and (6) two sites within the Bron Fm. near Saint Barthélémy. From *Cassinis et al.* [2003], modified and redrawn.

[1991], *Zheng et al.* [1992], *Lethiers et al.* [1993], *Broutin and Durand* [1995], and *Gand and Durand* [2006].

2.1. Permian Stratigraphy

2.1.1. Les Pellegrins Formation

[7] The oldest unit, the 50 to 80 m-thick Les Pellegrins Formation unconformably overlies the metamorphic basement throughout the Toulon-Cuers basin. It starts with a conglomerate/breccia unit containing mainly basement-derived phyllitic clasts, followed by an alternation of thick grey to yellow sandstone lenses representing fluvial channel-fills and thinner dark-grey silt and clay layers pertaining to floodplain deposits. Red hues are very localized and siderite nodules and lenses are frequent.

[8] The age of the Les Pellegrins Formation is broadly constrained between the Stephanian and the middle-late Autunian (~299–282 Ma) [*Parent*, 1932; *Bouillet and Lutaud*, 1958; *Basso*, 1987; *Ronchi et al.*, 1998]. The transition to the overlying unit, the Transy Formation (not sampled for paleomagnetic investigation), is marked by an angular unconformity reaching up to 15°. The lower part of the Transy Formation consists of pale conglomeratic sandstones with high mineralogical maturity whereby most clasts are made of quartz.

2.1.2. Bron Formation

[9] The Bron Formation, located stratigraphically above the Transy Formation and exposed near Carnoules and Pignans (St. Barthélémy) is characterized by a variably thick sequence of alternating arkosic sandstones, siltstones and red to greenish clays. Tuff deposits associated with rhyolitic lava flows are also present. According to its stratigraphic position, the Bron Formation can be dated to post-Stephanian to pre-Kungurian (~299–275 Ma).

2.1.3. Les Salettes Formation

[10] The Les Salettes Formation is highly heterogeneous in composition; the lower member comprises tuffs associated with more than 7 basaltic lava flows that reach local thicknesses between 10 and 40 m. These flows, outcropping in the Carqueiranne area, pertain to the second Permian magmatic (alkaline) cycle of the Western Mediterranean [*Leroy and Cabanis*, 1993]. The remainder of the lower member consists of coarse- to medium-grained sandstones and conglomerates with volcanic clasts arranged in low-angle, cross-stratified tabular sets pertaining to braided river

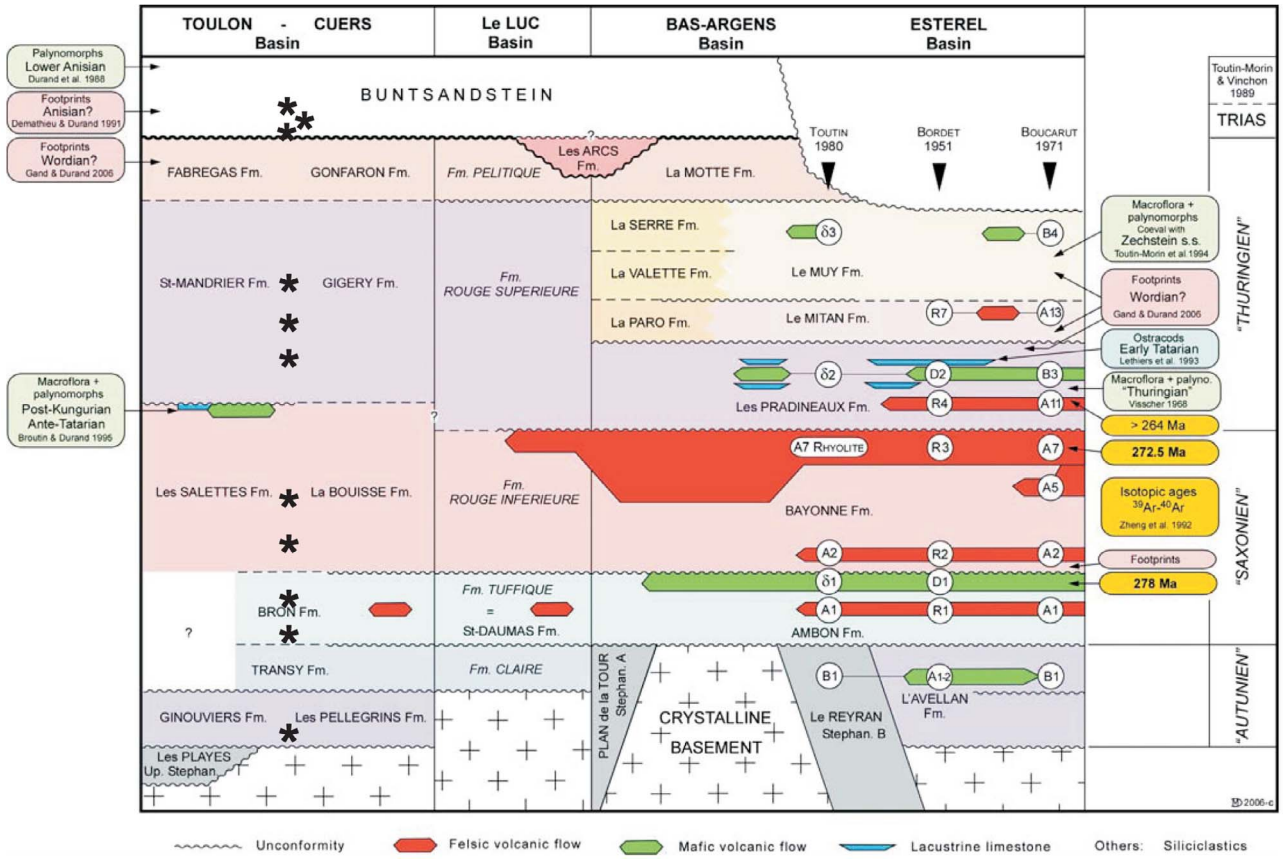

Figure 4. Lithostratigraphic correlations through the Permian basins of Provence with location of the dating elements. Asterisks indicate the position of the sampled horizons. After *Durand* [2008] and references therein.

settings. The upper member of the Les Salettes Formation, the Bau Rouge Limestone, crops out along the cliffs of Cap Garonne. It was defined by *Durand* [1993] as a 25 m-thick unit consisting of limestone beds of mainly lacustrine environment with domal stromatolites and black chert nodules. Macroscopic plant remains and palynomorphs led *Broutin and Durand* [1995] to suggest a post-Kungurian to pre-Tatarian age for the Bau Rouge member.

2.1.4. Saint-Mandrier Formation

[11] The Permian Saint-Mandrier Formation reaches a total thickness of about 700 m [see *Durand*, 2008, p. 706]. The upper part of the section contains 7 rhyolitic tuff beds that present the last phase of Permian volcanic activity in Provence. Sediments of meandering-channel settings are also present [*Durand*, 1993]; according to sedimentological evidence, these sediments were deposited by bed-load, medium-scale streams under mild to semi-arid climate conditions [*Durand*, 1993].

2.1.5. Gonfaron Formation

[12] The 40 m-thick Gonfaron Formation represents the uppermost part of the Permian sequence within the Toulon-Cuers basin (coeval to the Fabregas Formation as shown in Figure 4). It consists of a rather monotonous succession of red claystones and siltstones interlayered with green, thinly bedded and fine-grained sandstones with sedimentary structures like current and wave ripples, desiccation cracks, and small load casts. Trace fossils were described by *Demathieu et al.* [1992].

2.2. Triassic Stratigraphy

2.2.1. Buntsandstein Group

[13] Two formations have been defined within the Buntsandstein Group of Provence: the basal Poudingue de Port-Issol Formation and the Grès de Gonfaron Formation [*Glinzboeckel and Durand*, 1984; *Durand*, 1988]. The 8 m-thick Poudingue de Port-Issol is a grain supported oligomictic conglomerate consisting mainly of quartz pebbles and small cobbles derived from quartz veins with silicious matrix. It is well exposed to the south of Port-Issol Point, Fabregas and Carqueiranne Point. Its high mineralogical and textural maturity speak in favor of protracted, maybe even polycyclic, fluvial transport. Many pebbles also display secondary edges due to abrasion by wind-blown sand and thus testify to arid climates, recognized also in other parts of Europe around the middle part of the Scythian (Early Triassic) [*Durand et al.*, 1989].

[14] The 12 m-thick Grès de Gonfaron Formation (not to be confused with the Permian Gonfaron Formation) is mainly comprised of coarse- to medium-grained grey-greenish to red sandstones, locally alternating with claystones (e.g., near Plage de la Garonne), pertaining to floodplain to playa settings. The presence of frequent carbonate

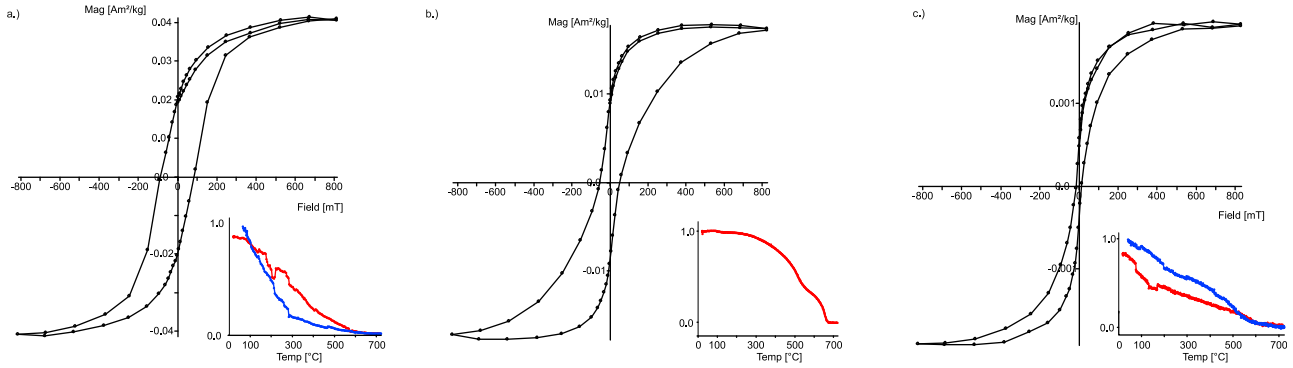

Figure 5. Hysteresis curve for (a) one of the Les Salettes tuff samples, (b) one of the Saint-Mandrier tuff samples and (c) one of the Saint-Mandrier redbed samples. The thermomagnetic curves are plotted with normalized intensities.

concretions of pedogenic origin and, in the upper part, of paleosols (dolocretes, silicretes) indicate arid to semi-arid climates [*Durand et al.*, 1989]. The Grès de Gonfaron Formation is dated to the early Anisian (∼245 Ma) based on palynomorphs [*Durand*, 1988, and references therein]. In the study area, the Grès de Gonfaron strata are tilted up to 80° as a consequence of tectonic activity related to the Pyrenean-Provençal orogeny (mainly Paleocene to Early Eocene in age) that lead to N-S shortening in the Toulon region (M. Durand, personal communication, 2011).

2.2.2. Muschelkalk Group

[15] Along the Triassic belt of Provence, the Grès de Gonfaron Formation is overlain by the Grès en plaquettes de Solliès Formation attributed to the Muschelkalk Group [*Durand*, 2001]. It consists of yellowish grey sandstones containing halite pseudomorphs that are considered as the first evidence of post-Variscan marine influence in the area [*Durand*, 2001].

3. Field and Laboratory Methods

[16] A total of 150 oriented core samples were taken from 14 sites at six locations (Figure 3); 108 samples yielded reliable paleomagnetic component directions, described hereafter. In stratigraphic order, the sampled rock units are: (1) Les Pellegrins Fm., (2) Bron Fm., (3) Les Salettes Fm., (4) Saint-Mandrier Fm., (5) Poudingue de Port-Issol Fm. and (6) Grès de Gonfaron Fm. Within each formation, several sites were drilled in the field with a gasoline-powered, water-cooled rock-drill and oriented using a standard magnetic compass; samples were then labeled with an univocal code containing the formation name acronym, e.g. MAN for the Saint-Mandrier Fm., followed by the site number (1, 2, ..). Individual samples taken at each site are again numbered, such that sample 1 from site 1 from the St. Mandrier Formation is labeled MAN1-1.

[17] Subsequently all samples were in the laboratory cut into ∼10 cc cylindrical specimens. Multiple specimens cut from one sample were used to provide checks on the consistency of the natural remanent magnetization (NRM) and on additional rock-magnetic measurements.

[18] All samples were studied in the paleomagnetic laboratory of the University of Munich. The specimens were stepwise thermally demagnetized using a Schoenstedt oven. The magnetization was measured with a 2G Enterprises DC-SQUID (Superconducting QUantum Interference Device) cryogenic magnetometer in a magnetically shielded room. Hysteresis parameters were determined using a Variable Field Translation Balance (VFTB) [*Krasa et al.*, 2007]. Pilot studies demonstrated that thermal demagnetization is more efficient than alternating field demagnetization, and thus the vast majority of the specimens was thermally demagnetized using increments of 20–30°C up to maximum temperatures of 690°C. Demagnetization results were plotted on orthogonal vector diagrams [*Zijderveld*, 1967] and analyzed using the least squares method [*Kirschvink*, 1980] on linear portions of the demagnetization paths defined by at least four consecutive demagnetization steps. The linear fits were anchored to the origin of the demagnetization axes where appropriate. Only occasionally the combined use of remagnetization circles and endpoint data [*McFadden and McElhinny*, 1988] was applied to retrieve component directions with overlapping coercivity spectra. Subsequently, site mean directions were calculated from the paleomagnetic directions of the individual samples. Thus, it was possible to calculate a virtual geomagnetic pole for each site.

4. Rock-Magnetic Data

[19] Rock-magnetic measurements were performed on selected samples representative of the main studied lithologies (Figure 5). All tuff samples from the Les Salettes Formation show very similar rock-magnetic behaviors (Figure 5a). Key features of the heating portion of the thermomagnetic experiments are (a) a drop in intensity at ∼150–180°C, followed by (b) an increase in intensity at ∼230–250°C and (c) a final decrease in intensity observed at ∼575°C. The cooling portion of the thermomagnetic experiments does not follow the heating curve below ∼575°C whereby it reveals much lower intensities. The hysteresis measurements suggest the presence of a single magnetic phase that tends to saturate at fields of around 600mT (Figure 5a).

Table 1. Site Characteristics, Paleomagnetic Data, Site Mean Directions and Virtual Geomagnetic Pole Positions From This Study[a]

Site Characteristics						In Situ			Bedding Corrected			VGP Location	
Name	Age[b] (Ma)	Formation[c]	GLat	GLon	N/N′	D°	I°	α_{95}	D°	I°	α_{95}	PLat	PLon
BAR1	285 ± 10	tuff	43.49	6.36	6/9	188.6	−23.0	3.9	180.1	−18.1	3.9	−56.3	5.8
BAR2	285 ± 10	tuff	43.49	6.36	6/7	50.4	5.1	37.9	49.3	11.3	37.9	−32.8	302.1
BRO	285 ± 10	red sdst	43.30	6.19	13/14	208.2	−10.5	6.4	199.1	−16.3	6.4	−51.5	334.7
SAL1[d]	273 ± 2.6	cgl	43.09	6.07	4/7	–	–	–	–	–	–	–	–
SAL2	273 ± 2.6	ext ig	43.09	6.07	13/19	236.6	−49.4	9.4	232.4	−24.6	9.4	−36.0	293.4
SAL3	273 ± 2.6	tuff	43.09	6.07	3/4	239.0	−54.8	7.8	220.5	−9.3	7.8	−37.6	311.2
MAN1	260 ± 10	tuff	43.08	5.9	4/6	183.4	−33.9	5.1	181.1	−21.7	5.1	−58.2	4.0
MAN2	260 ± 10	tuff	43.08	5.9	7/11	179.1	−29.1	4.0	176.8	−19.3	4.1	−56.8	11.8
MAN3	260 ± 10	tuff	43.08	5.9	5/7	179.4	−29.4	2.6	175.4	−20.8	2.6	−57.5	14.4
MAN4	260 ± 10	red sdst	43.08	5.9	7/8	178.5	−21.4	3.9	170.2	−21.1	4.0	−56.8	23.8
MAN5	260 ± 10	red sdst	43.08	5.9	4/6	180.6	−20.6	41.3	172.4	−24.7	41.6	−59.2	20.6
GAR1	243 ± 2.9	grey and red sdst	43.09	6.03	6/8	50.6	−70.5	13.3	184.8	−28.9	13.3	−62.1	356.1
GAR2	243 ± 2.9	grey and red sdst	43.09	6.03	6/12	171.9	81.1	30.7	10.6	15.3	23.8	−53.4	346.8
GAR3	243 ± 2.9	grey and red sdst	43.09	6.03	10/16	212.3	75.6	10.9	17.9	24.1	10.9	−55.9	333.7

[a]GLat/GLon: geographic latitude/longitude of sampling site; N/N′: number of analyzed samples/total amount of samples; D°/I°: paleomagnetic declination/inclination; α_{95}: circle of 95% confidence; PLat/PLon: latitude/longitude of virtual geomagnetic pole. All VGPs are mirrored to the southern hemisphere for better visualization. Stratigraphic age estimates come from *Durand* [2006, 2008, and references therein].

[b]The stratigraphic ages were transformed into numerical ages using the International Stratigraphic Chart with listed numerical ages from *Gradstein et al.* [2005] and *Ogg et al.* [2008].

[c]Abbreviations: sdst – sandstone, cgl – conglomerate, ext ig – extrusive igneous rocks.

[d]Conglomerate test, no mean direction.

[20] The wasp-waisted shape of the hysteresis curves of the Saint-Mandrier tuff samples (Figure 5b) implies the coexistence of two phases with contrasting coercivity spectra [*Jackson et al.*, 1990; *Tauxe et al.*, 1996]. Based on the thermomagnetic curves, these two magnetic phases are interpreted as magnetite and heamatite with Curie temperatures [*Moskowitz*, 1981] of ∼570°C and ∼660°C, respectively.

[21] The thermomagnetic curves of sandstone and redbed samples from the Saint-Mandrier Formation (Figure 5c) commonly display intensity drops at ∼575°C, close to the Curie temperature of magnetite. Minor amounts of a higher coercivity phase are also inferred from the hysteresis loops that display a slightly wasp-waisted shape (Figure 5c).

5. Paleomagnetic Data

[22] Characteristic component (ChRM) directions retrieved from the investigated stratigraphic units are discussed hereafter; site mean directions and the associated VGPs are summarized in Table 1.

5.1. Bron Formation

[23] The Permian Bron Formation was sampled at three sites (BAR1, BAR2, BRO; Table 1) from two localities (#5 and #6 in Figure 3) near the town of Carnoules and near Pignans (St. Barthélémy). The orthogonal projection diagrams (Figure 6a) clearly show the presence of two components; a lower temperature viscous component successfully isolated up to ∼200°C is usually followed by a higher temperature component oriented to the south-and-up and trending toward the origin of the orthogonal projection at up to 690°C. The high temperature ChRM component is used to calculate site mean directions listed in Table 1 and plotted on Figure 8 before and after bedding tilt correction. The ChRM site mean direction from site BAR2 at St. Barthélémy (Table 1) is characterized by a very high α_{95} of 37.9° and was therefore excluded from further analysis.

5.2. Les Salettes Formation

[24] The Permian Les Salettes Formation was sampled at three sites (SAL1, SAL2, SAL3; Table 1) to the east of the town of Toulon (#3 in Figure 3). Here, samples from a conglomerate horizon, from igneous extrusives, and from tuff deposits were taken. The conglomerate samples were used to perform a conglomerate test (Figure 7).

[25] The detailed thermal demagnetization experiments performed on the samples from the Les Salettes Formation show at least two components with overlapping unblocking spectra, indicated by the curved shape of the orthogonal vector end point projections (Figure 6b). As can be seen from the normalized intensity decay plot, the low temperature component carries more than 80% of the magnetization intensity and was successfully removed by heating up to ∼300°C (Figure 6b, inset). The high temperature ChRM direction points toward the southwest with negative inclinations (Figure 6b); the associated site mean directions (Table 1) are plotted on Figure 8 before and after bedding tilt correction. Because of the homogeneous bedding attitude at these sites, and because the rocks only display reverse polarity, it was not possible to perform a fold or reversal test. However, paleomagnetic results based on four samples from the polymictic conglomerate at site SAL1 show widely dispersed paleomagnetic directions which are taken as evidence for a primary age of magnetization (Figure 7).

5.3. Saint-Mandrier Formation

[26] Five sites were drilled within the Permian Saint-Mandrier Formation (sites MAN1, MAN2, MAN3, MAN4, MAN5; Table 1) near the harbor of St. Mandrier (#1 in Figure 3). The demagnetization behavior of the samples is characterized by an initial NRM intensity increase up to ∼200°C due to the removal of a low temperature component, followed by a gradual intensity decrease up to ∼660°C

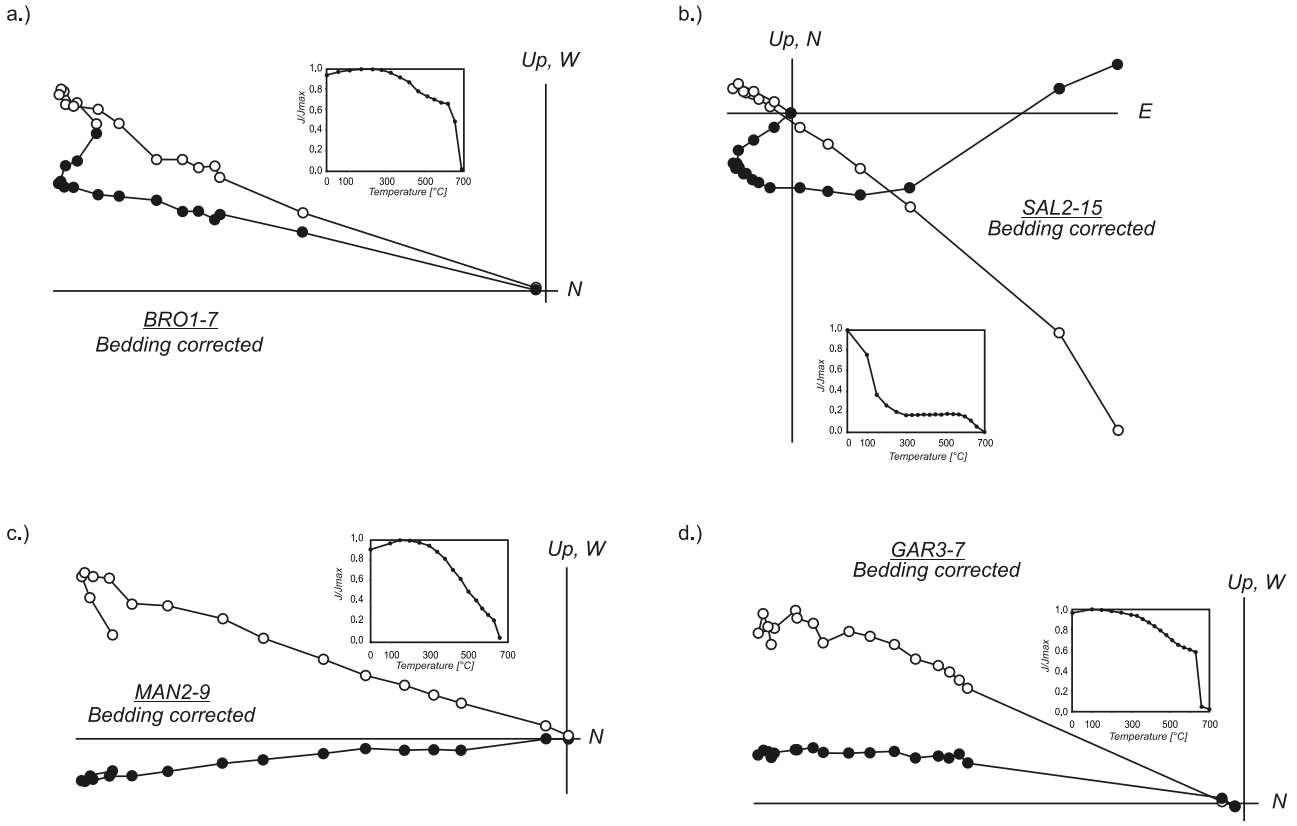

Figure 6. (a–d) Results of thermal demagnetization experiments plotted as orthogonal vector diagrams [*Zijderveld*, 1967] in stratigraphic coordinates together with normalized diagrams of intensity decay. Full (open) dots represent vector endpoints projected onto the horizontal (vertical) plane. For clarity NRM values are not plotted.

(Figure 6c). The high temperature ChRM component is consistently oriented toward the south with negative inclinations (Figure 6c). The resulting ChRM site mean directions (Table 1), characterized by low α_{95} values ($\leq 5.1^\circ$, saved for site MAN5), are plotted on Figure 8 before and after bedding tilt correction.

5.4. Grès de Gonfaron Formation

[27] Three sites from the Triassic grey to red sandstones of the Grès de Gonfaron Formation (sites GAR1, GAR2, GAR3; Table 1) sampled at the Cap de la Garonne (#2 in Figure 3) showed during thermal demagnetization the presence of two distinct magnetic component directions. A slight increase in NRM intensity upon removal of a low temperature viscous overprint up to $\sim 100^\circ$C is followed by a continuous intensity decrease up to $\sim 660^\circ$C associated with a dual polarity ChRM component direction oriented either to the north-and-down or to the south-and-up after correction for bedding tilt (Figure 6d). The ChRM site mean directions (Table 1) are plotted in Figure 9 before and after bedding tilt correction. A reversal test performed on the ChRM directions from the N = 22 samples of the three sites resulted positive and classified as 'C' after *McFadden and McElhinny* [1990], confirming the primary character of the isolated ChRM component (Figure 9).

5.5. Data Summary

[28] Permian and Triassic site mean directions are shown in Figures 8 and 9, respectively. The Permian site mean directions show consistently negative inclinations, pointing toward the S-SW after bedding tilt correction; a conglomerate test performed in the Les Sallettes Formation revealed randomly distributed paleomagnetic directions indicating that the isolated ChRM is primary in origin. High temperature characteristic palaeomagnetic directions of dual polarity were identified in the Triassic samples. The primary character of the ChRM of these rocks was confirmed by a positive reversal test.

6. Interpretation

[29] The following main observations and interpretations can be drawn from the paleomagnetic data outlined above.

[30] 1. The Early Permian paleopoles derived from our data show a clear distribution along a small circle that was calculated using the least squares method (standard deviation of 4.1°) (Figure 10). This distribution indicates similar paleolatitudes for the studied rocks at the time of their formation. Published poles from the Corso-Sardinian block (Table 2) [*Edel*, 2000, and references therein] were rotated to European coordinates using the rotation parameters of *van*

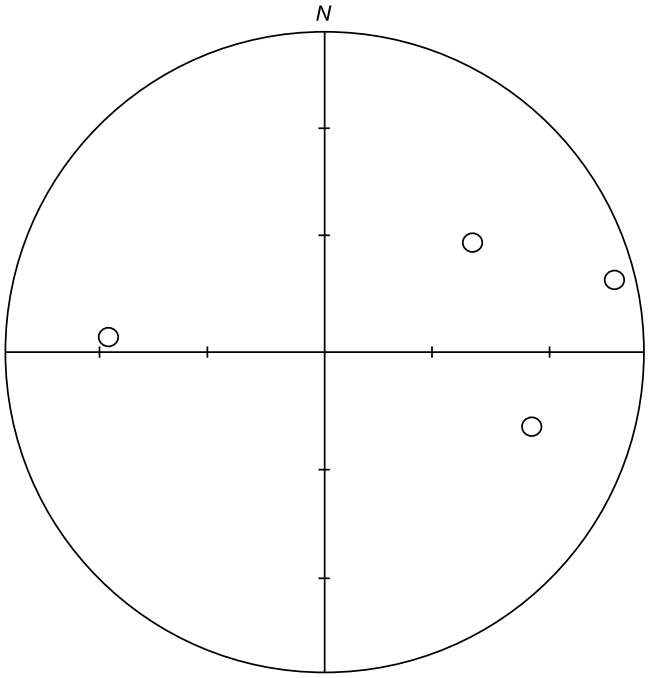

Figure 7. Paleomagnetic results based on four samples from a polymictic conglomerate from the Les Salettes Formation show a widely distributed directional data set which might be taken as evidence for a primary age of magnetization. Open symbols indicate negative inclinations.

der Voo [1969] and *Gattacceca et al.* [2007]. These rotated poles (Table 3) as well as the poles from the Maures-Estérel region (Table 2) [*Edel*, 2000] also plot on this small circle (Figure 10).

[31] 2. The inclinations measured in samples from different sites do not show any statistically significant scatter. This is in clear contrast with the wide range of observed declinations, indicating true relative rotations between the individual blocks.

[32] 3. The small circle that fits the distribution of paleopoles intersects the APWP of Baltica [*Smethurst et al.*, 1998] in the Early Permian (~290–260 Ma), in good agreement with the stratigraphic ages of the sampled units.

[33] 4. The Early Permian paleopoles from this study plot on either side of the Baltica APWP, indicating clockwise and counterclockwise relative rotations of the studied crustal blocks with respect to stable Europe.

[34] 5. The observed block rotations of the crustal blocks can be accounted for by a single, mean Euler pole located in Western Europe (Figure 10). This indicates that these block rotations occurred largely about vertical axes and broadly within the shear zones *sensu Arthaud and Matte* [1977] or *Muttoni et al.* [1996, 2003].

[35] 6. The Triassic poles from this study (GAR) of Scythian to early Anisian age (~250–245 Ma), plot close to one another and close to the 250–240 Ma portion of the Baltica APWP (Figure 10). A main implication of this observation is that the observed block rotations were largely terminated before the Early Triassic rocks acquired their remanence.

[36] In summary, on the basis of our data, we suggest the existence in the Toulon-Cuers Basin of various tectonic blocks that rotated by different amounts and sense during a relatively narrow and well-defined time window straddling from sometime after the Early Permian (age of rotated rocks) and before the Early Triassic (age of non rotated rocks).

7. Discussion and Conclusions

[37] These findings are discussed in conjunction with data from the literature in quest for possible triggering mechanisms associated with Pangea instability and transformation during the late Paleozoic. To the west of the study area, a very similar timing of block rotations was observed in the Brive and Saint-Affrique basins of the French Massif Central

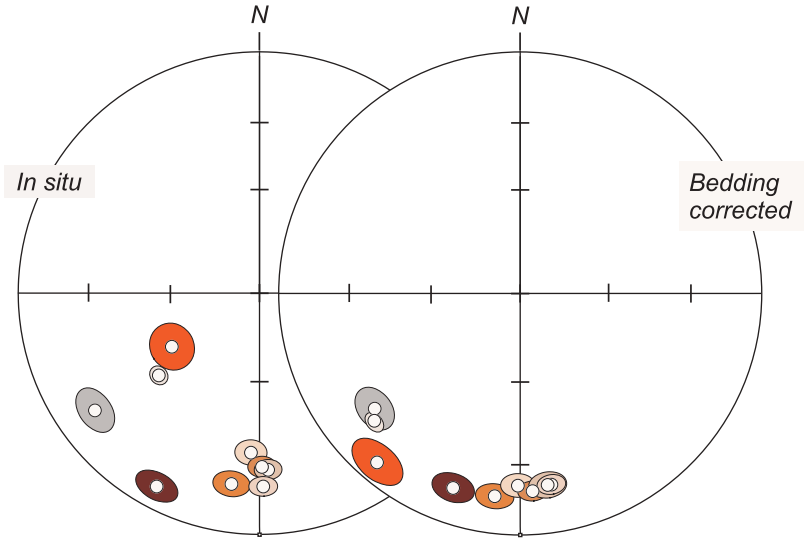

Figure 8. Stereographic projections of all Permian site mean directions in in situ and bedding corrected coordinates. Open symbols indicate negative inclinations.

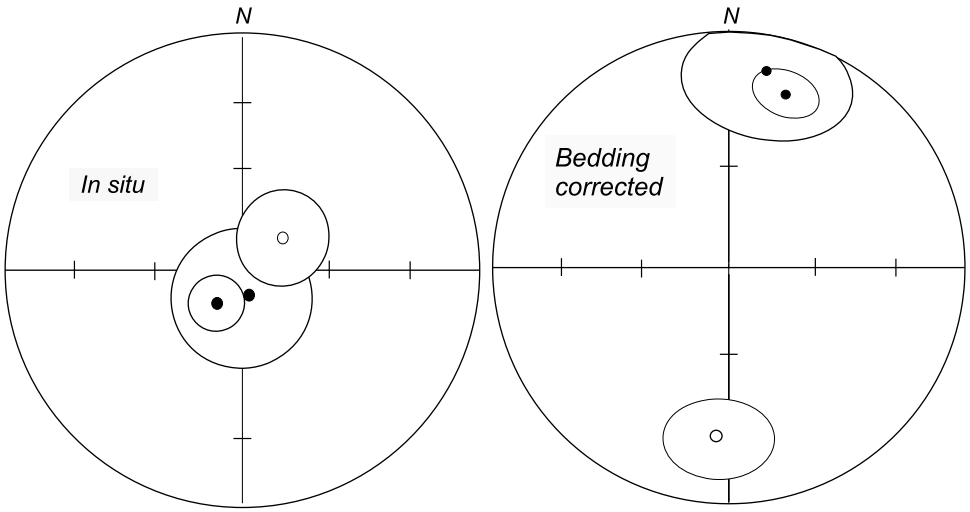

Figure 9. Stereographic projections of all Triassic site mean directions in in situ and bedding corrected coordinates. Open (closed) symbols indicate negative (positive) inclinations.

where Early Permian rocks show rotated paleomagnetic vectors while Late Permian rocks have not been affected by rotations [*Chen et al.*, 2006; see also *Cogné et al.*, 1990, 1993; *Diego-Orozco and Henry*, 1998; *Henry et al.*, 1999; *Diego-Orozco et al.*, 2002]. Paleomagnetic data from the Maures-Estérel massif located immediately to the east of our study area suggest a large clockwise block rotation during the Early to Middle Permian [*Edel*, 2000]. A recent

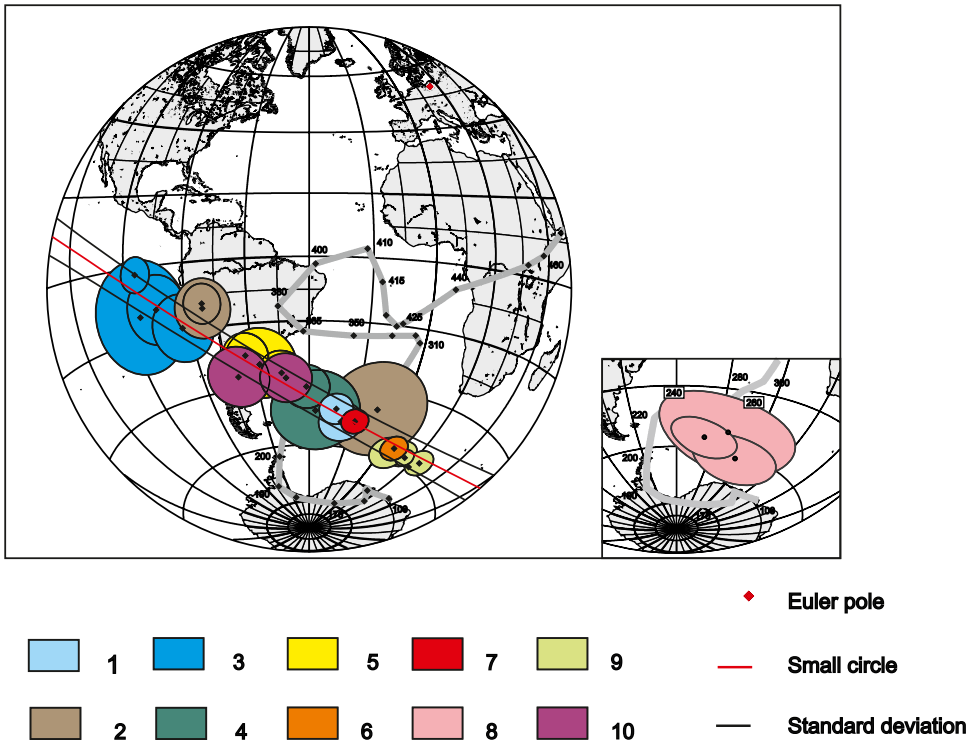

Figure 10. 1–5: Virtual geomagnetic poles from previous studies (Tables 2 and 3); 6–10: Virtual geomagnetic poles from this study (Table 1) with respect to the apparent polar wander path of Baltica [*Smethurst et al.*, 1998]. The poles plot on a small circle about a Euler pole in present-day northwest Europe. Legend: (1) Estérel, (2) Maures, (3) N Corsica, (4) NW Sardinia, (5) S. Corsica–N. Sardinia, (6) BAR, (7) BRO, (8) GAR, (9) MAN, (10) SAL. The inset shows the three Triassic virtual geomagnetic poles from this study (calculated from paleomagnetic mean directions from sites GAR1, GAR2 and GAR3).

Table 2. Paleomagnetic Results and VGPs for the Late Carboniferous–Permian Formations of the Maures-Estérel-Corsica-Sardinia Block, Taken From *Edel* [2000][a]

Formations	Age (Ma)	Reference	N	D/I	Dc/Ic	α_{95}	Age Mag.	VGP (°N/°E)	Reference
				Maures					
Pelitic rocks	255 ± 5	*Merabet and Daly* [1986]	10	206/−31	196/−14	4	255	51/161	*Merabet and Daly* [1986]
Rhyolites	305 ± 5	*Begassat* [1985]	2	241/4	239/−16	–	–	–	*Zijderveld* [1975]
Rhyolites	305 ± 5	*Begassat* [1985]	7	240/−20	255/−5	6	290-280	14/105	*Edel* [2000]
–	305 ± 5	*Begassat* [1985]	5	254/−7	247/3	9	290-280	14/105	*Edel* [2000]
Rhyolite + Congl.	305 ± 5	*Begassat* [1985]	3	192/2	203/−22	15	280-260	44/170	*Edel* [2000]
Arcose	300	*Zijderveld* [1975]	1	198/−18	205/0	–	280-260	41/153	*Zijderveld* [1975]
				Estérel					
Basalts + Rhyolites	278 − 264	*Zheng et al.* [1992]	12	207/−9	207/−23	6	250-220	51/142	*Zijderveld* [1975]
Sediments	–	–	3	204/3	203/−12	5	250	47/150	*Zijderveld* [1975]
				N. Corsica					
Ignimbrites (1st cycle)	–	–	5	–	165/4	7	280-260	44/209	*Westphal et al.* [1976]
Ignimbrites (2nd cycle)	–	–	5	–	180/−29	16	250-220	64/189	*Westphal* [1976]
Dykes	–	–	16	177/−20	–	10	250-220	58/194	*Westphal* [1976]
Dolerites	–	–	–	167/−16	–	10	250-220	54/211	*Westphal* [1976]
Gabbro	290 ± 10	*Edel et al.* [1981]	–	189/−13	–	5	250-220	54/174	*Westphal* [1976]
				NW Sardinia					
Ignimbrites	303 ± 9	*Edel et al.* [1981]	2	124/24	126/−1	–	280-260	2/253	*Edel et al.* [1981]
Sdst.	Permo-Trias	*Edel et al.* [1981]	5	128/−7	120/−12	13	250-240	26/262	*Edel* [1980]
				S. Corsica–N. Sardinia					
Dykes	–	–	11	135/−11	–	7	280-260	36/250	*Vigliotti et al.* [1990]
Dykes	–	–	11	133/−2	–	7	280-260	31/249	*Vigliotti et al.* [1990]
Ignimbrites	288 ± 11	*Del Moro et al.* [1975]	6	142/3	142/−2	11	280-260	38/239	*Zijderveld et al.* [1970]
Ignimbrites	288 ± 11	*Del Moro et al.* [1975]	4	147/3	–	7	280-260	37/238	*Westphal* [1976]

[a]Age: age of the formation followed by the corresponding reference; N: number of sites; D/I: in situ declination/inclination; Dc/Ic: dip-corrected declination/inclination; Age mag.: assumed magnetization age; Reference: reference of the paleomagnetic study. This table shows unrotated poles.

palaeomagnetic study on Permo-Carboniferous dykes of Sardinia [Emmer et al., 2005] revealed significant counterclockwise rotations of up to 64° between individual parts of the island that have been demonstrated to predate the Jurassic [*Kirscher et al.*, 2011].

[38] Summarizing the above, paleomagnetic data seem to indicate the existence of an intra-Pangea belt of tectonic blocks straddling from the Massif Central to southern France and Corsica-Sardinia (and speculatively extending eastward to the north of Adria) characterized by complex and differential block rotations that—based on data from Toulon-Cuers—may have largely occurred in post-Early Permian and pre-Early Triassic times. Taken at face value, this timing seems to preclude an origin of the postulated block belt as consequence of dextral wrench tectonics *sensu Arthaud and Matte* [1977], which occurred in the Late Carboniferous–Early Permian and therefore seemingly predated block belt activity in the Middle Permian, as we speculate here. We notice instead that the timing of the Pangea B [*Irving*, 1977] to Pangea A transformation broadly agrees with the timing of block rotation documented in this study. The transformation occurred essentially during the Middle Permian from an Early Permian Pangea B to a Late Permian Pangea A [*Muttoni et al.*, 1996, 2003, 2009].

[39] Pangea B remains however a strongly debated issue that received considerable attention in the recent years, as briefly (and probably incompletely) summarized hereafter. *Domeier et al.* [2011c] argued against an intra-Pangea transform zone in the Late Permian–Early Triassic but admitted that Pangea B could not be ruled out in the Late Carboniferous–Early Permian, thus confirming previous findings [*Muttoni et al.*, 1996, 2003; *Angiolini et al.*, 2007]. More recently, *Domeier et al.* [2011a] reprised *Rochette and Vandamme* [2001] in stressing that significant inclination shallowing in sediments would result in inaccurate reconstruction of paleolatitudes, therefore artificially generating the crustal overlap between Laurasia and Gondwana

Table 3. Paleopoles for Corsica-Sardinia From the Literature Rotated to European Coordinates, Using Rotation Parameters of *Gattacceca et al.* [2007] and *van der Voo* [1969] and Projected to the Southern Hemisphere as Plotted in Figure 10

Age Mag.[a] (Ma)	α_{95}	VGP (°N/°E)	Reference[b]
	S. Corsica–N. Sardinia		
280-260	7	−36/310	*Vigliotti et al.* [1990]
280-260	7	−38/311	*Vigliotti et al.* [1990]
280-260	11	−33/302	*Zijderveld et al.* [1970]
280-260	7	−30/298	*Westphal* [1976]
	N. Corsica		
280-260	7	−16/285	*Westphal et al.* [1976]
250-220	16	−14/264	*Westphal* [1976]
250-220	10	−12/270	*Westphal* [1976]
250-220	10	−19/278	*Westphal* [1976]
250-220	5	−2/264	*Westphal* [1976]
	NW Sardinia		
280-260	7	−41/319	*Edel et al.* [1981]
250-240	13	−48/323	*Edel* [1980]

[a]Age mag.: assumed magnetization age.
[b]Reference: reference of the paleomagnetic study. References always refer to the unrotated and unprocessed poles.

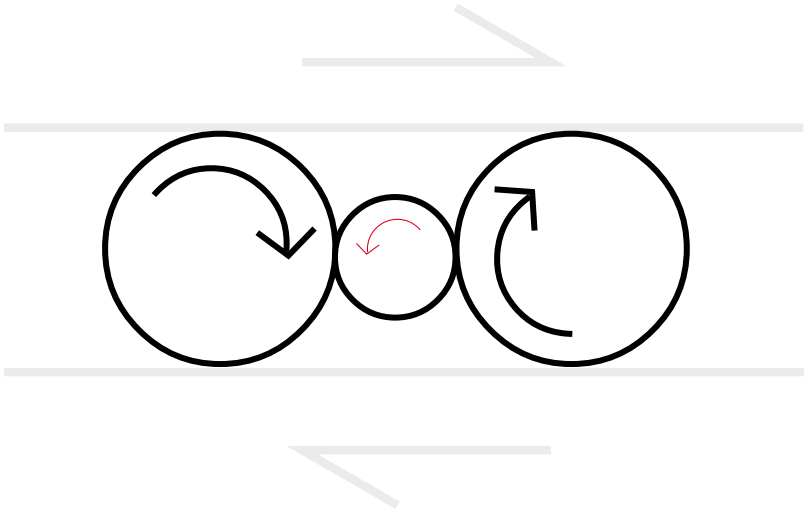

Figure 11. Simple ball bearing model to explain the observed differential rotations.

on which the Pangea B concept is based, which was however found by *Muttoni et al.* [2003] in igneous rocks that are usually not affected by inclination shallowing. Recent paleomagnetic data from Argentina and Norway re-confirmed Pangea A in the Late Permian-Triassic [*Domeier et al.*, 2011b, 2011c; *Dominguez et al.*, 2011], while *Yuan et al.* [2011] in their study on Permian and Triassic paleolatitudes of the Ukrainian shield concluded that both Pangea B and A are allowed in the Early Permian depending on data selection. More recently, *Domeier et al.* [2012] showed in their comprehensive review that selected paleomagnetic data from the literature can be reconciled with Pangea A also in the Early Permian without invoking non-dipole field contributions (as previously done by *van der Voo and Torsvik* [2001] and *Torsvik and van der Voo* [2002]; see also *Muttoni et al.* [2003] for a discussion); however, we notice that this conclusion (no Pangea B in the Early Permian) was reached [*Domeier et al.*, 2012] by excluding—with little circumstantial explanation—Early Permian data from Adria retrieved [*Muttoni et al.*, 1996, 2003] from rocks that (i) are igneous and therefore not affected by sedimentary inclination shallowing, (ii) pertain to well known stratigraphic and geologic contexts characterized by low tectonic deformation, (iii) have been carefully dated with modern radiometric techniques, (iv) yielded well illustrated and good quality paleomagnetic directions from sites confined to one hemisphere (greatly reducing the possible effects of zonal non-dipole field contaminations on Pangea geometry as previously suggested; see above), and, finally, (v) yielded paleomagnetic poles that agree with available poles from Africa of arguably same age, testifying for substantial tectonic coherence of Adria and Africa, which was incidentally observed also for the Triassic, Jurassic, Cretaceous, and Cenozoic [*Muttoni et al.*, 1996, 2003]. Forty years of work on selected rocks from stable parts of Adria that frequently yielded paleomagnetic data of high *van der Voo*'s [1990] Q quality and showed ~280 Myr of history of substantial tectonic coherence with Africa [e.g., *Channell*, 1996; *Muttoni et al.*, 1996, 2003] have been largely excluded from the road of reconciliation to Pangea [*Domeier et al.*, 2012].

[40] Finally, a reconstruction of the Early Permian stress field of Iberia from the analysis of the curved Cantabria-Asturias arc was used to question the likeliness of dextral shearing associated with the Pangea B to A transformation in the Early Permian [*Weil et al.*, 2001], but we recall that subsequent analysis placed the transformation largely in the middle part of the Permian [*Muttoni et al.*, 2003], a period for which no stress field reconstruction is available to our knowledge.

[41] While the issue of Pangea B will probably be resolved paleomagnetically by retrieving new and reliable Early Permian data [*Yuan et al.*, 2011], we stress that the 'critically lacking' [*Domeier et al.*, 2012] geological evidence for the major dextral shear between Laurasia and Gondwana required for the Pangea B to A transformation may in fact be represented by the belt of rotated blocks described in this study. The presence within this block belt of counterclockwise rotations (e.g., in Sardinia) as well as of opposite-sense rotations (e.g., in the Toulon-Cuers basin) may seem counterintuitive in a dextral megashear regime, which would predict essentially clockwise rotations. However, *Lamb* [1987] convincingly demonstrated that the sense of rotation of crustal blocks trapped in a major shear zone very much depends on strain rate, aspect ratio, interaction of blocks, and boundary conditions along the shear zone. Additional examples from the literature show that different amounts of clockwise and counterclockwise rotations of blocks can co-exist under common strike-slip regimes [e.g., *Ron et al.*, 1984]. We use a simple configuration of two larger blocks with a smaller block caught in between to illustrate the concept (Figure 11). In such an assemblage, small clockwise rotations of the larger blocks would cause large counterclockwise rotations of the intervening small block. As our paleomagnetic data indicate that blocks rotated by different amounts, and because the size of the blocks is considerably smaller than that of the transform zone, we adopted as more realistic the model developed by *McKenzie and Jackson* [1983], which would result in a block arrangement similar to that illustrated in Figure 12. Acknowledging the lack of fundamental information about block outlines, aspect ratio of blocks, and interaction among

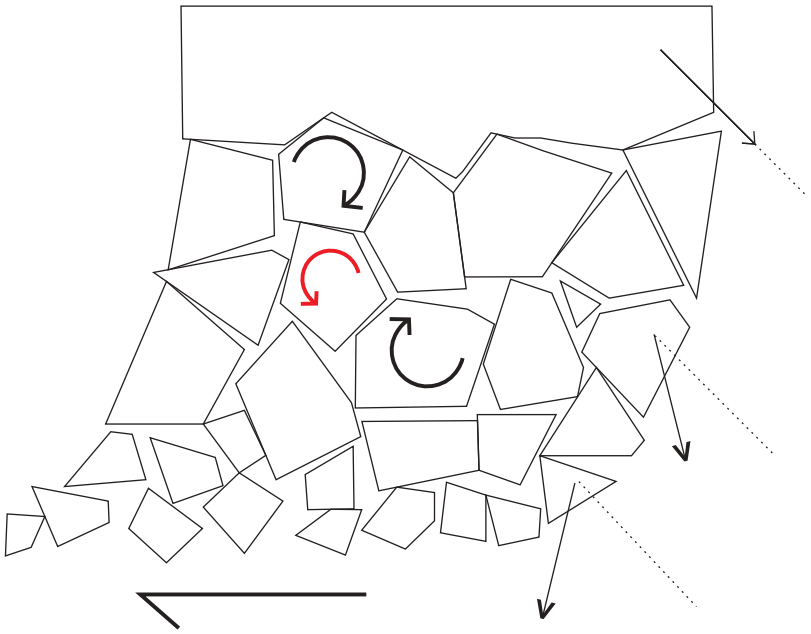

Figure 12. The small block model as proposed by *McKenzie and Jackson* [1983]. The brittle upper crust is broken into small blocks which rotate in response to the continuous, ductile deformation at greater depth. Notice the interaction between single blocks. Redrawn and modified after *Nelson and Jones* [1987]. Small black arrows on the right represent the direction of an ancient magnetization direction.

blocks, the adopted model (Figure 12) well illustrates that the dextral motion of Laurasia relative to Gondwana could have been largely taken up by and distributed among differential rotations of several fault-bounded crustal blocks rather than by a set of discrete, continental-scale shear zones. To our knowledge, there is no theoretical upper limit to the amount of (dextral) displacement that can be taken up by the postulated block belt, which could range from the ~600 km proposed by *Arthaud and Matte* [1977] to the ~3000 km associated with the Pangea B to A transformation.

[42] **Acknowledgments.** Paleomagnetic sampling in the Toulon-Cuers basin was carried out by Barbara Emmer and Alexandra Abalmassava. Thanks to Manuela Weiss for support during rock- and paleomagnetic measurements. Financial support to VB by the German Research Foundation (DFG grant Ba1210/8-1) is gratefully acknowledged. We thank Rob van der Voo for useful comments and for sharing with us his views and opinions while allowing us to maintain ours; further thanks goes to an anonymous reviewer for detailed and constructive comments on the manuscript.

References

Angiolini, L., M. Gaetani, G. Muttoni, M. H. Stephenson, and A. Zanchi (2007), Tethyan oceanic currents and climate gradients 300 m. y. ago, *Geology*, *35*, 1071–1074.

Arthaud, F., and P. Matte (1977), Late Paleozoic strike-slip faulting in southern Europe and northern Africa: Result of a right-lateral shear zone between the Appalachians and the Urals, *Geol. Soc. Am. Bull.*, *88*, 1305–1320.

Aubele, K., V. Bachtadse, and G. Muttoni (2009), Paleogeographic reconstructions in the Mediterranean - A paleomagnetic study of Jurassic sediments from Sardinia, *Eos Trans. AGU*, *90*(22), Jt. Assem. Suppl., Abstract GP11F-02.

Bard, J. P. (1997), Démembrement anté-mésozoïque de la chaîne varisque d'Europe occidentale et d'Afrique du Nord: rôle essentiel des grands décrochements transpressifs dextres accompagnant la rotation-translation horaire de l'Afrique durant le Stéphanien, *C. R. Acad. Sci., Ser. IIa*, *324*, 693–704.

Basso, A.-M. (1987), Les formations carbonifères de la Provençe orientale (Sud-Est de la France), *Geol. Alp.*, *13*, 19–24.

Begassat, P. (1985), Les bassins stéphaniens des Maures et de Tanneron; pétrologie, géochimie du volcanisme, métallogénie, PhD thesis, 163 pp., Univ. Paris VI, Paris.

Bouillet, G., and L. Lutaud (1958), Contribution à l'étude paléogéographique de la période permienne dans la Provence cristalline, *Bull. Soc. Geol. Fr.*, *8*(5), 447–462.

Broutin, J., and M. Durand (1995), First paleobotanical and palynological data on the "Les Salettes Formation" uppermost member (Permian Toulon Basin, Southeastern France), paper presented at XIIIth International Congress on the Carboniferous and Permian, Pol. Geol. Inst., Krakow, Poland.

Cassinis, G., M. Durand, and A. Ronchi (2003), Permian-Triassic continental sequences of Northwest Sardinia and South Provence: Stratigraphic correlations and palaeogeographical implications, *Bull. Soc. Geol. Ital.*, *2*, 119–129.

Channell, J. E. T. (1996), Palaeomagnetism and palaeogeography of Adria, in *Palaeomagnetism and Tectonics of the Mediterranean Region*, edited by A. Morris and D. H. Tarling, *Geol. Soc. Spec. Publ.*, *105*, 119–135.

Chen, Y., B. Henry, M. Faure, J.-F. Becq-Giraudon, J.-Y. Talbot, L. Daly, and M. Le Goff (2006), New Early Permian paleomagnetic results from the Brive basin (French Massif Central) and their implications for Late Variscan tectonics, *Int. J. Earth Sci.*, *95*, 306–317.

Cogné, J. P., J. P. Brun, and J. Van den Driessche (1990), Paleomagnetic evidence for rotation during Stephano-Permian extension in southern Massif Central (France), *Earth Planet. Sci. Lett.*, *101*, 272–280

Cogné, J. P., J. Van den Driessche, and J. P. Brun (1993), Syn-extension rotations in the Permian St Affrique basin (Massif Central, France): Paleomagnetic constraints, *Earth Planet. Sci. Lett.*, *115*, 29–42.

Del Moro, A., P. Di Simplicio, C. Ghezzo, G. Guasparri, F. Rita, and G. Sabatini (1975), Radiometric data and intrusive sequence in the Sardinia batholith, *Neues Jahrb. Mineral., Abh.*, *126*, 28–44.

Demathieu, G., and M. Durand (1991), Les traces de pas de Tétrapodes dans le Trias détritique du Var et des Alpes maritimes (France), *Bull. Mus. Natl. Hist. Nat., Sect. C*, *13*, 115–133.

Demathieu, G., G. Gand, and N. Toutin-Morin (1992), La palichnofaune des bassins permiens provençaux, *Geobios*, *25*(1), 19–54

Diego-Orozco, A., and B. Henry (1998), Palaeomagnetic data from the Permian Rodez basin and rotations in the southwestern border of the Massif Central, *C. R. Acad. Sci., Ser. IIa*, *327*, 225–229.

Diego-Orozco, A., Y. Chen, B. Henry, and J.-F. Becq-Giraudon (2002), Paleomagnetic results from the Permian Rodez basin implications: The Late Variscan tectonics in the southern French Massif Central, *Geodin. Acta*, *15*, 249–260.

Domeier, M., R. Van der Voo, and F. B. Denny (2011a), Widespread inclination shallowing in Permian and Triassic paleomagnetic data from Laurentia: Support from new paleomagnetic data from Middle Permian shallow intrusions in southern Illinois (USA) and virtual geomagnetic pole distributions, *Tectonophysics*, *511*, 38–52.

Domeier, M., R. Van der Voo, E. Tohver, R. N. Tomezzoli, H. Vizan, T. H. Torsvik, and J. Kirshner (2011b), New Late Permian paleomagnetic data from Argentina: Refinement of the apparent polar wander path of Gondwana, *Geochem. Geophys. Geosyst.*, *12*, Q07002, doi:10.1029/2011GC003616.

Domeier, M., R. Van der Voo, R. N. Tomezzoli, E. Tohver, B. W. H. Hendriks, T. H. Torsvik, H. Vizan, and A. Dominguez (2011c), Support for an "A-type" Pangea reconstruction from high-fidelity Late Permian and Early to Middle Triassic paleomagnetic data from Argentina, *J. Geophys. Res.*, *116*, B12114, doi:10.1029/2011JB008495.

Domeier, M., R. Van der Voo, and T. Torsvik (2012), Paleomagnetism and Pangea: The road to reconciliation, *Tectonophysics*, *514–517*, 14–43.

Dominguez, A. R., R. Van der Voo, T. H. Torsvik, B. W. H. Hendriks, A. Abrajevitch, M. Domeier, B. T. Larsen, and S. Rousse (2011), The ~270 Ma palaeolatitude of Baltica and its significance for Pangea models, *Geophys. J. Int.*, *186*, 529–550.

Durand, M. (1988), Le Trias détritique du "Bassin du Sud-Est": Paléogéographie et environnements de dépôt, *Geol. Alp. Mem.*, *14*, 69–78.

Durand, M. (1993), Un exemple de sédimentation continental permienne dominée par l'activité de chenaux méandriformes: La formation de Saint-Mandrier (Bassin de Toulon, Var), *Geol. Fr.*, *2*, 43–55.

Durand, M. (2001), The continental Permian-Triassic series of Provence (southeast France): Field trip guidebook of the International Field Conference on the Stratigraphic and Structural Evolution of the Late Carboniferous to Triassic Continental and Marine Successions in Tuscany (Italy). Regional reports and general correlations, report, 29 pp., Univ. di Siena, Siena, Italy.

Durand, M. (2006), The problem of the transition from the Permian to the Triassic Series in southeastern France: Comparison with other Peritethyan regions, in *Non-Marine Permian Biostratigraphy and Biochronology*, edited by S. G. Lucas, G. Cassinis, and J. W. Schneider, *Geol. Soc. Spec. Publ.*, *265*, 281–296.

Durand, M. (2008), Permian to Triassic continental successions in southern Provence (France): An overview, *Boll. Soc. Geol. Ital.*, *127*(3), 697–716.

Durand, M., G. Avril, and R. Meyer (1988), Paléogéographie des premiers depôts triasiques dans les Alpes externes méridionales: Importance de la Dorsale delphino-durancienne, *C. R. Acad. Sci. Paris, Ser. II*, *306*, 557–560.

Durand, M., R. Meyer, and G. Avril (1989), *Le Trias Détritique de Provence, du dome de Barrot et du Mercantour*, *Publ. Assoc. Sedimentol. Fr.*, vol. 6, 135 pp., Bordeaux, France.

Edel, J.-B. (1980), Etude paléomagnétique en Sardaigne. Conséquences pour la géodynamique de la Méditerranée occidentale, PhD thesis, 310 pp., Strasbourg I, Strasbourg, France.

Edel, J.-B. (2000), Hypothèse d'une ample rotation horaire tardi-varisque du bloc Maures-Estérel-Corse-Sardaigne, *Geol. Fr.*, *1*, 3–19, 2000.

Edel, J. B., R. Montigny, and R. Thuizat (1981), Late Paleozoic rotations of Corsica and Sardinia: New evidence from paleomagnetic and K-Ar studies, *Tectonophysics*, *79*, 201–223.

Emmer, B., V. Bachtadse, G. Muttoni, A. Ronchi, and D. V. Kent (2005), Paleomagnetism of Late Paleozoic Dyke Swarms from Sardinia, *Eos Trans. AGU*, *86*(52), Fall Meet. Suppl., Abstract GP11A-0015.

Gand, G., and M. Durand (2006), Tetrapod footprint ichnoassociations from French Permian basins: Comparisons with other Euramerican ichnofaunas, in *Non-Marine Permian Biostratigraphy and Biochronology*, edited by S. G. Lucas, G. Cassinis, and J. W. Schneider, *Geol. Soc. Spec. Publ.*, *265*, 157–177.

Gattacceca, J., A. Deino, R. Rizzo, D. S. Jones, B. Henry, B. Beaudoin, and F. Vadeboin (2007), Miocene rotation of Sardinia: New paleomagnetic and geochronological constraints and geodynamic implications, *Earth Planet. Sci. Lett.*, *258*, 359–377.

Glinzboeckel, C., and M. Durand (1984), Provence et chaines subalpines méridionales, in *Synthèse Géologique du Sud-Est de la France*, vol. 1, *Stratigraphie et Paléogéographie*, *Mem. BRGM*, vol. 125, edited by S. Debrand-Passard, S. Courbouleix, and M.-J. Lienhardt, pp. 99–100, Bur. de Rech. Geol. et Min., Orleans, France.

Gradstein, F. M., J. G. Ogg, and A. G. Smith (Eds) (2005), *A Geologic Time Scale*, Cambridge Univ. Press, Cambridge, U. K.

Henry, B., J.-F. Becq-Giraudon, and H. Rouvier (1999), Paleomagnetic studies in the Permian Basin of Largentière and implications for the Late Variscan rotations in the French Massif Central, *Geophys. J. Int.*, *138*, 188–198.

Irving, E. (1977), Drift of the major continental blocks since the Devonian, *Nature*, *270*, 304–309.

Irving, E. (2005), The role of latitude in mobilism debates, *Proc. Natl. Acad. Sci. U. S. A.*, *102*(6), 1821–1828.

Jackson, M., H.-U. Worm, and S. Banerjee (1990), Fourier analysis of digital hysteresis data: Rock magnetic applications, *Phys. Earth Planet. Inter.*, *65*, 78–87.

Kirscher, U., K. Aubele, G. Muttoni, A. Ronchi, and V. Bachtadse (2011), Paleomagnetism of Jurassic carbonate rocks from Sardinia: No indication of post-Jurassic internal block rotations, *J. Geophys. Res.*, *116*, B12107, doi:10.1029/2011JB008422.

Kirschvink, J. L. (1980), The least-square line and plane and the analysis of paleomagnetic data, *Geophys. J. R. Astron. Soc.*, *62*, 699–718.

Krasa, D., K. Petersen, and N. Petersen (2007), Variable field translation balance, in *Encyclopedia of Geomagnetism and Paleomagnetism*, edited by D. Gubbins and E. Herrero-Bervera, pp. 977–979, Springer, Dordrecht, Netherlands.

Lamb, S. H. (1987), A model for tectonic rotations about a vertical axis, *Earth Planet. Sci. Lett.*, *84*, 75–86.

Leroy, S., and B. Cabanis (1993), Le volcanisme permien du bassin de Toulon: Un jalon septentrional du volcanisme permien de l'Ouest méditerranéen, *Geol. Fr.*, *2*, 57–66.

Lethiers, F., R. Damotte, and J. Sanfourche (1993), Premières données sur les ostracodes du permien supérieur continental de l'Estérel (SE de la France): Systématique, biostratigraphie, paléoécologie, *Geol. Mediterr.*, *20*(2), 109–125.

McCann, T., C. Pascal, M. J. Timmermann, P. Krzywiec, J. López-Gómez, A. Wetzel, C. M. Krawczyk, H. Rieke, and J. Lamarche (2006), Post-Variscan (end Carboniferous–Early Permian) basin evolution in western and central Europe, *Eur. Lithosphere Dyn.*, *32*, 355–388.

McFadden, P., and M. McElhinny (1988), The combined analysis of remagnetization circles and direct observations in palaeomagnetism, *Earth Planet. Sci. Lett.*, *87*, 161–172.

McFadden, P., and M. McElhinny (1990), Classification of the reversal test in paleomagnetism, *Geophys. J. Int.*, *103*, 725–729.

McKenzie, D. P., and J. A. Jackson (1983), The relationship between strain rates, crustal thickening, paleomagnetism, finite strain, and fault movement within a deforming zone, *Earth Planet. Sci. Lett.*, *65*, 182–202.

Merabet, N., and L. Daly (1986), Détermination d'un pôle paléomagnétique et mise en évidence d'aimantations à polarité normale sur les formations du Permien supérieur du Massif des Maures (France), *Earth Planet. Sci. Lett.*, *80*, 156–166.

Moskowitz, B. M. (1981), Methods for estimating Curie Temperatures of Titanomaghemites from experimental J_s-T Data, *Earth Planet. Sci. Lett.*, *53*, 84–88.

Muttoni, G., D. V. Kent, and J. E. T. Channell (1996), Evolution of Pangea: paleomagnetic constraints from the Southern Alps, Italy, *Earth Planet. Sci. Lett.*, *140*, 97–112.

Muttoni, G., D. V. Kent, E. Garzanti, P. Brack, N. Abrahamsen, and M. Gaetani (2003), Early Permian Pangea B to Late Permian Pangea A, *Earth Planet. Sci. Lett.*, *215*, 379–394.

Muttoni, G., D. V. Kent, E. Garzanti, P. Brack, N. Abrahamsen, and M. Gaetani (2004), Erratum to "Early Permian Pangea B to Late Permian Pangea A", *Earth Planet. Sci. Lett.*, *218*, 539–540.

Muttoni, G., M. Gaetani, D. V. Kent, D. Sciunnach, L. Angiolini, F. Berra, E. Garzanti, M. Mattei, and A. Zanchi (2009), Opening of the Neo-Tethys Ocean and the Pangea B to Pangea A transformation during the Permian, *GeoArabia*, *14*(4), 17–48.

Nelson, M. R., and C. H. Jones (1987), Paleomagnetism and crustal rotations along a shear zone, Las Vegas Range, Southern Nevada, *Tectonics*, *6*(1), 13–33, doi:10.1029/TC006i001p00013.

Ogg, J. G., G. Ogg, and F. M. Gradstein (2008), *The Concise Geologic Time Scale*, Cambridge Univ. Press, Cambridge, U. K.

Parent, H. (1932), Le terrain houllier à Collobrières et en environs d'Hyères, *C. R. Somm. Seances Soc. Geol. Fr.*, *11*, 159–161.

Rochette, P., and D. Vandamme (2001), Pangea B: An artifact of incorrect paleomagnetic assumptions?, *Ann. Geofis.*, *44*(3), 649–658.

Ron, H., R. Freund, Z. Garfunkel, and A. Nur (1984), Block rotation by strike-slip faulting: Structural and paleomagnetic evidence, *J. Geophys. Res.*, *89*, 6256–6270, doi:10.1029/JB089iB07p06256.

Ronchi, A., J. Broutin, J. B. Diez, B. Freytet, J. Galtier, and F. Lethiers (1998), New palaeontological discoveries in some Early Permian sequences of Sardinia. Biostratigraphic and palaeogeographic implications, *C. R. Acad. Sci., Ser. IIa*, *327*, 713–719.

Smethurst, M. A., A. N. Khramov, and S. Pisarevsky (1998), Paleomagnetism of the Lower Ordovician Orthoceras Limestone, St. Petersburg, and a revised drift history for Baltica in the early Palaeozoic, *Geophys. J. Int.*, *133*, 44–56.

Tauxe, L., T. A. T. Mullender, and T. Pick (1996), Potbellies, wasp-waists, and superparamagnetism in magnetic hysteresis, *J. Geophys. Res.*, *101*, 571–583, doi:10.1029/95JB03041.

Toutin-Morin, N., and C. Vinchon (1989), Les bassins permiens du Sud-Est, in *Synthèse Géologique des Bassins Permiens Français*, *Mem.*

BRGM, vol. 128, edited by J.-J. Chateauneuf and G. Farjanel, pp. 114–121, Bur. de Rech. Geol. et Min., Orleans, France.

Toutin-Morin, N., et al. (1994), Notice explicative: Carte géologique de la France à 1/50000, feuille Fréjus-Cannes, feuille 1024, Bur. Rech. Geol. Min, Orléans, France.

Torsvik, T. H., and R. van der Voo (2002), Refining Gondwana and Pangea paleogeography: Estimates of Phanerozoic non-dipole (octupole) fields, *Geophys. J. Int.*, *151*, 771–794.

van der Voo, R. (1969), Paleomagnetic evidence for the rotation of the iberian peninsula, *Tectonophysics*, *7*, 5–56.

van der Voo, R. (1990), The reliability of paleomagnetic data, *Tectonophysics*, *184*, 1–9.

van der Voo, R., and T. H. Torsvik (2001), Evidence for late Paleozoic and Mesozic non-dipole fields provides an explanation for the Pangea reconstruction problems, *Earth Planet. Sci. Lett.*, *187*, 71–81.

Vigliotti, L., W. Alvarez, and M. O. McWilliams (1990), No relative rotation detected between Corsica and Sardinia, *Earth Planet. Sci. Lett.*, *98*, 313–318.

Visscher, H. (1968), On the Thuringian age of the Upper Palaeozoic sedimentary and volcanic deposits of the Estérel, Southern France, *Rev. Palaeobot. Palynol.*, *6*, 71–83.

Weil, A. B., R. Van der Voo, and B. A. Van der Pluijm (2001), Oroclinal bending and evidence against the Pangea megashear: The Cantabria-Asturias arc (northern Spain), *Geology*, *29*(11), 991–994.

Westphal, M. (1976), Paléomagnetisme des formations permiennes de Corse. Comparaison avec la Sardaigne et l'Estérel, *Bull. Soc. Geol. Fr.*, *18*(5), 1209–1215.

Westphal, M., J. Orsini, and P. Vellutini (1976), Le micro-continent corso-sarde, sa position initiale: données paleomagnétiques et raccords géologiques, *Tectonophysics*, *30*, 141–157.

Yuan, K., R. Van der Voo, M. L. Bazhenov, V. Bakhmutov, V. Alekhin, and B. W. H. Hendriks (2011), Permian and Triassic palaeolatitudes of the Ukrainian shield with implications for Pangea reconstructions, *Geophys. J. Int.*, *184*, 595–610.

Zheng, J., J.-F. Mermet, N. Toutin-Morin, J. Hanes, A. Gondolo, R. Morin, and G. Feraud (1992), Datation 40Ar-39Ar du magmatisme et de filons minéralisés permiens en Provence orientale (France), *Geodin. Acta*, *5*(3), 203–215.

Zijderveld, J. D. A. (1967), A. C. demagnetization of rocks: Analysis of results, in *Methods in Paleomagnetism*, edited by D. W. Collinson, K. M. Creer, and S. K. Runcorn, pp. 254–286, Elsevier Sci., New York.

Zijderveld, J. D. A. (1975), Paleomagnetism of the Estérel rocks, PhD thesis, 199 pp., Utrecht Univ., Utrecht, Netherlands.

Zijderveld, J. D. A., K. A. De Jong, and R. van der Voo (1970), Datation of Sardinia: Paleomagnetic evidence from Permian rocks, *Nature*, *226*, 933–934.